Optical properties of metallodielectric photonic crystals

V. Yannopapas* and A. Modinos
Department of Physics, National Technical University of Athens, Zografou Campus, GR-157 80 Athens, Greece

N. Stefanou
University of Athens, Section of Solid State Physics, Panepistimioupolis, GR-157 84 Athens, Greece

(Received 28 January 1999)

We present a systematic examination of the optical properties of photonic crystals consisting of metallic particles (plasma spheres) arranged periodically in a host dielectric medium. We calculate exactly the transmission and absorption coefficients of light incident on a slab of the material as functions of the frequency of the incident light and analyze the results by reference to the properties of a single sphere and to the frequency band structure of the corresponding infinite crystal. We examine the dependence of the above coefficients on the fractional volume occupied by the spheres and on the thickness of the slab. Finally we compare our results with those of the Maxwell Garnett effective-medium theory and in this way we establish the limitations of the latter. We show in particular that multipole interactions which the Maxwell Garnett theory does not take into account lead to significant structure in the transmission/absorption spectra. [S0163-1829(99)15131-2]

I. INTRODUCTION

Composite films consisting of small metallic particles distributed periodically or randomly in a host dielectric medium have optical properties which are strikingly different from those of the bulk metal and have been for many years the object of many experimental and theoretical investigations,[1–4] mainly because of the possible technological applications, e.g. as coatings for solar energy absorbers.[5]

The theoretical problem of light scattering by a spherical body, which is large enough to be describable by a macroscopic dielectric function $\epsilon_S(\omega)$, and is situated in a homogeneous medium of different dielectric function $\epsilon(\omega)$ has been solved by Mie[6] and Debye[7] at the beginning of this century. When the wavelength of light is much larger than the diameter of the sphere, one obtains the following formula for its (dipolar) polarizability:[8]

$$\alpha(\omega)=\frac{3v}{4\pi}\frac{\epsilon_S-\epsilon}{\epsilon_S+2\epsilon}, \tag{1}$$

where v is the volume of the sphere.

When one deals with a periodic distribution of identical particles in a host medium, and for the case when the distance between the spheres is much smaller than the wavelength of light, the optical properties of the composite medium are usually described by an appropriate dielectric function in the manner of Maxwell Garnett.[9] Usually, the metallic spheres are replaced by Drude plasma spheres, i.e., $\epsilon_S(\omega)$ of Eq. (1) is approximated by

$$\epsilon_S(\omega)=1-\frac{\omega_p^2}{\omega(\omega+i\tau^{-1})}, \tag{2}$$

where ω_p stands for the bulk plasma frequency of the metal and τ is the relaxation time of the conduction band electrons. To obtain the electric dipole moment induced on an individual sphere, in accordance with Eqs. (1) and (2), one needs to calculate the *local field* at the given sphere, which one does, using the Clausius-Mossotti equation (one assumes that the spheres are centered on a cubic lattice). Once the local field has been calculated, and the dipole moment induced on a single sphere obtained through Eq. (1), the polarization of the composite medium and the corresponding dielectric function of this medium, denoted by $\bar{\epsilon}(\omega)$, is calculated using standard formulas of electrostatics. We obtain

$$\frac{\bar{\epsilon}-\epsilon}{\bar{\epsilon}+2\epsilon}=f\frac{\epsilon_S-\epsilon}{\epsilon_S+2\epsilon}, \tag{3}$$

where f is the fractional volume occupied by the spheres. The above equation is referred to in the literature as the Maxwell Garnett (MG) equation. The electrostatic (dipole) approximation underlying the derivation of Eq. (3) remains valid for a random distribution of particles, but a formula for the dielectric function of the composite medium is more difficult to obtain in that case.[10]

In recent years a number of methods have been developed which allow one to solve, more or less exactly, Maxwell's equations in a photonic crystal consisting of dielectric or metallic spheres (large enough to be describable by a real or complex dielectric function) arranged periodically in a host medium of different dielectric function. The considerable activity in this area of research is motivated to a large degree by the possibility of having non-absorbing materials with (absolute) photonic gaps; i.e., regions of frequency over which light cannot exist within the crystal,[11,12] which in turn promises interesting technological applications.[13,14] Among the methods suggested for the calculation of the frequency band structure of a photonic crystal, the so-called on-shell methods are numerically efficient and at the same time allow the calculation of the transmission, reflection, and absorption coefficients of light, of given frequency, incident on a slab of the photonic crystal.[3,15,16] It is, therefore, now possible to calculate exactly the above-mentioned coefficients for a slab of a crystal (e.g., metal spheres in a host dielectric medium)

and compare with the respective results of an effective-medium theory. We have, in fact, already shown[15] that for small values of f the MG equation is accurate enough at low frequencies (below the first Bragg gap) for a non-absorbing cubic crystal of dielectric spheres embedded in a medium of different dielectric constant.

In the present paper we shall examine in some detail the optical properties of systems consisting of metallic spheres, with a relative dielectric function given by Eq. (2), arranged periodically (to begin with) in a nonabsorbing dielectric medium. We aim to clarify the physical picture underlying the optical processes under consideration, and by the way establish the limitations of an effective-medium approach as represented by the MG equation.

II. FREQUENCY BANDS AND TRANSMISSION COEFFICIENTS

We assume that identical spheres are centered on the lattice of a fcc crystal. We view the crystal as a stack of layers (planes of spheres) parallel to the (001) surface. For given $\mathbf{k}_\parallel$, the component of the reduced wave vector parallel to the (001) surface which lies in the surface Brillouin zone (SBZ) of the given surface, we can calculate the real frequency lines, $k_z = k_z(\omega, \mathbf{k}_\parallel)$, using the method described in Ref. 15. The details of the method and a computer program for its implementation can be found in Ref. 17. A frequency line gives the z component of the wave vector [normal to the (001) plane] as a function of the frequency ω, for the given $\mathbf{k}_\parallel$. The regions of ω over which k_z is real define corresponding frequency bands, and regions over which k_z is complex define corresponding frequency gaps (stop gaps). The corresponding solutions of Maxwell's equations [eigenmodes of the electromagnetic (EM) field in the infinite crystal] are Bloch waves: the electric-field component of the EM field (a similar equation is obeyed by the magnetic field) satisfies the equation

$$\mathbf{E}(\mathbf{r}+\mathbf{R}_n) = \exp(i\mathbf{k}\cdot\mathbf{R}_n)\mathbf{E}(\mathbf{r}), \tag{4}$$

where $\mathbf{R}_n$ is a vector of the fcc space lattice, and $\mathbf{k} = (\mathbf{k}_\parallel, k_z(\omega;\mathbf{k}_\parallel))$. When k_z is real we have a propagating solution, and when k_z is complex we have an evanescent wave which grows exponentially as $z \to \infty$ or as $z \to -\infty$. In the infinite crystal, of course, only propagating waves have a real existence. Using the periodicity of the band structure in the k_z direction, i.e., $\omega(k_z + |\mathbf{b}_3|;\mathbf{k}_\parallel) = \omega(k_z;\mathbf{k}_\parallel)$ where $\mathbf{b}_3$ is the primitive vector of the reciprocal lattice normal to the (001) plane, we define the reduced $\mathbf{k}$-zone appropriate to this surface as follows: $\mathbf{k} = (\mathbf{k}_\parallel, k_z)$, with $\mathbf{k}_\parallel$ in the SBZ and $-|\mathbf{b}_3|/2 \leqslant k_z < |\mathbf{b}_3|/2$.

In Fig. 1(a) we show the frequency bands for $\mathbf{k}_\parallel = 0$ [dispersion curves along the normal to the (001) plane] of a particular fcc crystal. The crystal consists of identical plasma spheres with a radius $S = 50$ Å, and a dielectric function defined by Eq. (2) with $\hbar\omega_p = 9.2$ eV which corresponds to the plasma frequency of bulk silver.[10] We assume, to begin with, that the spheres are nonabsorbing, i.e., $\tau = \infty$. We choose to plot the energy $\hbar\omega$ versus a normalized wave vector component $k_z a/2\pi$, where $a = 275.65$ Å is the lattice constant of the crystal which for the given value of S corresponds to a fractional volume occupied by the spheres $f = 0.1$. The medium

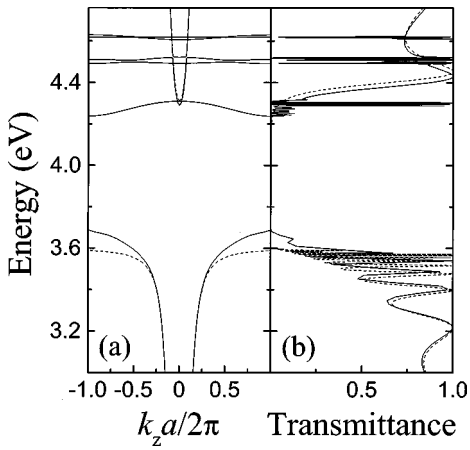

FIG. 1. (a) The photonic band structure associated with the (001) surface of a fcc crystal of nonabsorbing plasma spheres ($S = 50$ Å, $\hbar\omega_p = 9.2$ eV, $\tau = \infty$) in gelatine ($\epsilon = 2.37$) with $f = 0.1$, for $\mathbf{k}_\parallel = 0$. (b) The corresponding transmittance curve for light incident normally on a slab of the above crystal, 16-layers thick. The solid (broken) lines in both figures refer to the exact (effective-medium) treatment.

between the spheres (host medium) has a relative dielectric constant $\epsilon = 2.37$ (gelatine). All the bands shown in Fig. 1(a) are doubly degenerate and couple with light incident normally on a slab of the crystal parallel to the (001) surface. The continuous lines represent the frequency bands in the selected frequency region which result from the exact calculation as described above. There exist other [not shown in Fig. 1(a)], nondegenerate bands which do not couple with *normally* incident light; this is because the electric field in the corresponding eigenmodes of the EM field is carried by waves with wave vector components parallel to the surface $\mathbf{k}_\parallel + \mathbf{g} = \mathbf{g} \neq 0$, which cannot be matched with similarly propagating waves outside the crystal, for such do not exist [here we denote by $\mathbf{g}$ the two-dimensional reciprocal-lattice vectors corresponding to the surface under consideration; the (001) surface in the present case]. The existence of these optically inactive modes has been noted by a number of authors.[15,16,18,19] The broken lines in Fig. 1(a) show the dispersion curves one obtains from the effective-medium theory, i.e.,

$$\omega = \frac{c_0}{\sqrt{\bar{\epsilon}}} k_z, \tag{5}$$

where c_0 is the velocity of light in vacuum and $\bar{\epsilon}$ is given by Eq. (3). The nondegenerate bands obtained [but not shown in Fig. 1(a)] by the exact treatment cannot be obtained by an effective-medium theory. We shall give an example of such dispersion curves later on.

At this stage it is interesting to look for the physical origin of the frequency gap appearing in the diagram of Fig. 1(a), extending from $\omega \approx 3.68$ eV to $\omega \approx 4.24$ eV, in terms which are familiar in the energy band structure of electrons in ordinary crystals. For the qualitative analysis we have in mind, the effective-medium approach is sufficient. Using Eq. (2) with $\tau = \infty$, we can write Eq. (3) in the form

$$\bar{\epsilon} = C\left(\frac{A}{B}\right)^2 + \frac{C\omega_1^2[\epsilon - (A/B)^2]}{\omega_1^2 - \omega^2} \equiv \tilde{\epsilon} + \epsilon_r(\omega), \tag{6}$$

where

$$\omega_1 \equiv \omega_p / B,$$

$$C \equiv (1+2f)/(1-f),$$

$$A^2 \equiv \epsilon[1 + 2\epsilon(1-f)/(1+2f)],$$

$$B^2 \equiv 1 + \epsilon(2+f)/(1-f). \tag{7}$$

The physical meaning of Eq. (6) is made obvious as follows. We recall that the polarization **P** of the composite medium is given by

$$\mathbf{P} = \epsilon_0(\bar{\epsilon} - 1)\mathbf{E}, \tag{8}$$

where ϵ_0 is the dielectric constant of vacuum. In the present case the polarization has two components. The first component corresponds to the first term of Eq. (6). This does not depend on the frequency, and clearly the eigenmodes of the EM field corresponding to it will be described by a linear dispersion curve

$$\omega = \frac{c_0}{\sqrt{\tilde{\epsilon}}} k_z . \tag{9}$$

One can easily verify that when $f = 0$, the second term in Eq. (6) vanishes and the first term becomes $\tilde{\epsilon} = \bar{\epsilon}$. The second term in Eq. (6) is formally identical with an atomic resonance term. We note that when $f = 0$, we obtain from Eqs. (7) that $\omega_1 = \omega_p / \sqrt{1+2\epsilon}$ which is the dipole resonance of an isolated sphere according to Eq. (1). According to Eqs. (7) the interaction between the spheres shifts by a small amount the above resonance. Naturally this atomiclike resonance widens into a band of resonant states, but evidently the width of this band is very small and we can neglect it. If we were to disregard the coupling of this atomiclike band with the band of propagating states described by Eq. (9), we would obtain the flat band

$$\omega = \omega_1 . \tag{10}$$

The bands given by Eqs. (9) and (10) are shown by broken lines in Fig. 2. In reality the eigenmodes of the EM field result from a hybridization of states (of the same **k**) in the two bands and in this way a hybridization-induced gap opens up as shown by the solid lines representing the true (hybridized) eigenmodes of the EM field. We remember that these curves are obtained from Eq. (5). It is worth noting that hybridization is accomplished in the effective-medium treatment, by the way the dielectric function $\bar{\epsilon}$ enters into Eq. (5), namely as $\sqrt{\bar{\epsilon}}$, which in turn mixes in a particular manner the two terms of Eq. (6). Finally we note that the above remarks apply to those bands which are obtained by the effective-medium treatment.

Often, frequency gaps in photonic crystals, say dielectric spheres arranged periodically in a dielectric host medium, are the result of destructive interference between plane waves in the host medium scattered by the different spheres.

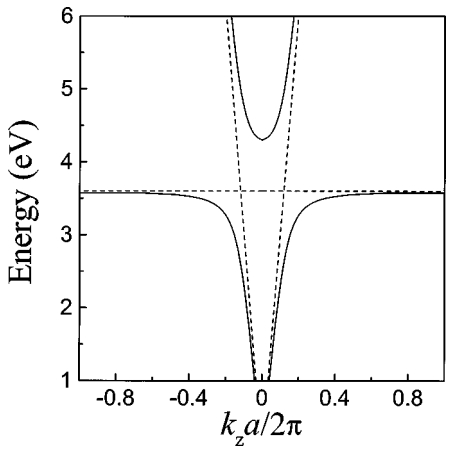

FIG. 2. The hybridization-induced gap in the photonic band structure of Fig. 1. The solid (broken) lines show the hybridized (unhybridized) bands, calculated in the effective-medium approximation.

Such gaps, known as Bragg gaps, cannot be reproduced by the MG theory. In the present case of metallodielectric crystals, the physical picture is somewhat different in the sense that the wavefield is better described by dipolar fields about the spheres which interact weakly between them and strongly with the propagating states given by Eq. (9) with which they hybridize in the manner described above to open the gap shown in Fig. 2. In relation to this gap the exact treatment amounts to an improved calculation of the local field acting on each sphere, but otherwise is similar to the picture underlying the MG approximation. The difference between the exact treatment and the MG one is more apparent at the bottom of the gap (see Fig. 1), where the presence of the pole in Eq. (6) makes the final result very sensitive to the method of calculation. We may add that the periodic structure is incidental in either approach (it is not necessary for the appearance of the gap), but it makes the calculation possible.

The flat bands above the gap, shown in Fig. 1(a), are due to higher multipole resonances of the individual spheres, and cannot be obtained by the effective-medium approximation. The eigenmodes of the EM field corresponding to these bands are strongly localized at the spheres and hybridize very weakly with the extended states. There is an infinite number of such bands, but only those corresponding to an angular momentum cutoff $\ell_{\max} = 4$ that we used in our calculation are shown in Fig. 1(a). The first flat band above the gap corresponds to $\ell = 2$, the next two flat bands correspond to $\ell = 3$ and the next two to $\ell = 4$. It is seen that, in the present case, apart from the flat bands and the nondegenerate ones mentioned above, the effective-medium approximation describes adequately the frequency band structure of the infinite crystal.

In Fig. 3 we show all the bands (including the nondegenerate ones) in the region about the $\ell = 3$ resonance. The nondegenerate bands, which as we have already mentioned do not couple with normally incident light, are shown by dotted lines. In the C_{4v} symmetry environment associated with normal incidence on the (001) surface of a cubic crystal, the sevenfold-degeneracy of an $\ell = 3$ resonance of a single sphere, splits into two doubly degenerate resonances and

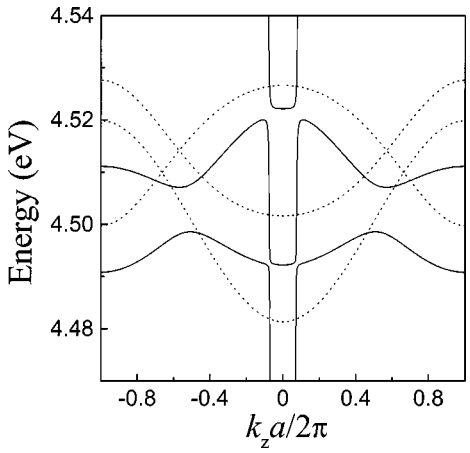

FIG. 3. The photonic band structure associated with the (001) surface of a fcc crystal of nonabsorbing plasma spheres ($S=50$ Å, $\hbar\omega_p=9.2$ eV, $\tau=\infty$) in gelatine ($\epsilon=2.37$) with $f=0.1$, for $\mathbf{k}_\parallel=0$, in the region about the $\ell=3$ resonance. The solid (dotted) lines refer to the doubly degenerate (nondegenerate) bands.

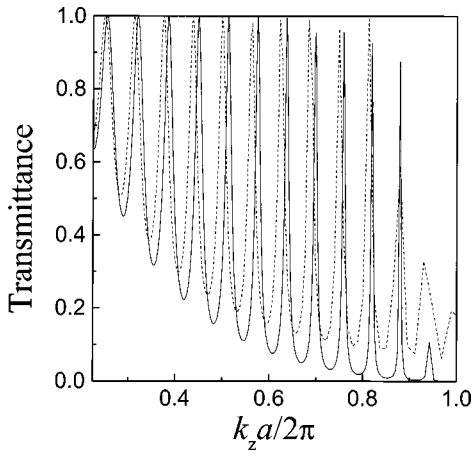

FIG. 4. The transmittance curve of Fig. 1(b), plotted as function of $k_z a/2\pi$, in a region below the band gap. The solid (broken) line refers to the exact (effective-medium) treatment.

three nondegenerate ones. The former give rise (in the crystal) to two doubly degenerate bands denoted by solid lines in Fig. 3, and the latter give rise to the above mentioned nondegenerate bands. We observe that only the degenerate bands hybridize with the band of continuum states which derive from Eq. (9), as expected from a group-theoretical analysis, giving rise to small frequency gaps.

Next to the frequency band structure in Fig. 1, we show the transmission coefficient of light incident normally on a slab of the crystal consisting of 16 planes of spheres parallel to the (001) surface. The medium on either side of the slab has the same dielectric constant $\epsilon=2.37$ as between the spheres of the slab. Again the agreement between the exact results (solid line) and the effective-medium ones (broken line) is good, except in the region of the flat bands above the gap. As expected, the transmission coefficient practically vanishes for frequencies within the frequency gap of the infinite crystal which extends from $\omega\approx3.68$ eV to $\omega\approx4.24$ eV. But the transmittance of a finite slab is not unity (or a nearly constant quantity) for the allowed (in the infinite crystal) frequencies. In both the exact and the effective-medium treatments one observes the oscillations in the transmittance one expects from the inteference of waves multiply reflected between the surfaces of the slab;[15,16] the peaks in the transmittance occurring when the effective half wavelength of the EM field in the slab, π/k_z, times an integer equals approximately the thickness, D, of the slab. In the present case $D\simeq Na/2$, where N is the number of layers in the slab and, therefore, one expects transmittance peaks when $k_z a/2\pi\simeq(n/N)$, where $n=1,2,\ldots,N-1$. This is demonstrated in Fig. 4. It must be noted that, for given ω, k_z for the exact result (solid line) is obtained from the exact dispersion curve as explained at the beginning of this section, whereas in the effective-medium treatment (broken line) k_z is obtained from Eq. (5). Since the two dispersion curves are not exactly the same, in a plot of transmittance versus frequency the transmittance peaks obtained in the effective-medium treatment will be displaced relative to those obtained in the exact treatment. However, in both cases the density of peaks (the number of peaks per unit frequency) increases considerably in the immediate vicinity of the frequency gap, and much more as one approaches the gap from below because of the flatness of the corresponding dispersion curve. Both these effects are apparent in Fig. 1. It is also evident from what we said above in relation to Fig. 4 that the number of transmittance peaks in any given frequency region will increase proportionally to the thickness of the slab.

III. ABSORBANCE

The absorbance of light by a slab of the composite material we have been considering is a quantity of great importance in many technological applications. We have so far suppressed it by putting $\tau=\infty$ in Eq. (2). In reality $\hbar\tau^{-1}\approx0.2$ eV or even greater. Absorption is associated mainly with the resonantly oscillating dipoles of the spheres and therefore most of it occurs mainly within a relatively short range of frequencies about ω_1. However, the existence of the frequency gap in the same region means that light does not propagate through the crystal when its frequency lies within the gap (the intensity of light decays exponentially into the crystal for these frequencies), and if it cannot enter into the crystal, it can not be absorbed either. It follows from the above that absorption will be significant at the edges of the gap, immediately below it and immediately above it. It appears that the higher ($\ell>1$) resonances above the gap (see Fig. 1) do not contribute significantly to absorption. We understand this as follows. In Fig. 5 we show the absorbance for increasing values of τ^{-1}, in the region of the $\ell=2$ resonance. When τ^{-1} is very small (a) we clearly see sharp absorption peaks associated with the $\ell=2$ resonance. As τ^{-1} increases, (a) to (b) to (c) to (d), the sharp resonances widen and eventually are submerged into the tail of the dipole ($\ell=1$) contribution to the absorbance. States of higher ℓ exhibit a similar behavior.

Let us first demonstrate the close relation between absorption and transmission. This is more clearly seen at low absorbance; we therefore put $\hbar\tau^{-1}=10^{-4}$ eV and calculate the transmission and absorption coefficients of light incident normally on a slab consisting of 4 and 32 planes of spheres, taking into account only the dipole contribution. The results are shown in Fig. 6. The solid lines show the transmission

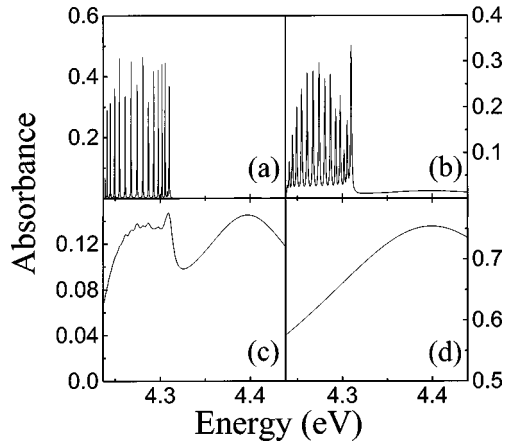

FIG. 5. Absorbance of light incident normally on a slab of 16 lattice planes parallel to the (001) surface of a fcc crystal, consisting of plasma spheres ($S=50$ Å, $\hbar\omega_p=9.2$ eV, $f=0.1$) in gelatine ($\epsilon=2.37$). The absorbance is shown in the energy region of the flat band of Fig. 1(a), associated with quadrupole resonant states, for different values of the relaxation time [(a) $\hbar\tau^{-1}=10^{-4}$ eV; (b) $\hbar\tau^{-1}=10^{-3}$ eV; (c) $\hbar\tau^{-1}=10^{-2}$ eV; (d) $\hbar\tau^{-1}=0.2$ eV]. Note the different scales for the different figures.

coefficient over an extended region of frequencies. In the insets we show the transmission (solid lines) and the absorption (broken lines) coefficient over the limited region of frequency where absorption occurs. A relatively large transmission coefficient implies that a relatively large fraction of light has gone through the slab, which implies a correspondingly high probability of it being absorbed. The insets in Fig. 6 show quite clearly that the absorbance peaks coincide with the transmission peaks. It is also evident that the magnitude of these peaks decays rapidly away from the gap edges. As we have already explained in the previous section, the number per unit energy of these peaks increases in the vicinity of the gap edges, more so near to the lower edge, and in proportion to the thickness of the slab. For the thinner slab (4-layers thick) there is no transmission peak above the gap, within the absorption range about ω_1, and therefore there is not an absorbance peak either. For the same slab there are a number of such peaks immediately below the gap. In the case of the thicker slab (32-layers thick), the number of transmission/absorption peaks below the gap, and within the absorption range about ω_1, increases considerably, and one sees the first two transmission/absorption peaks appearing above the gap.

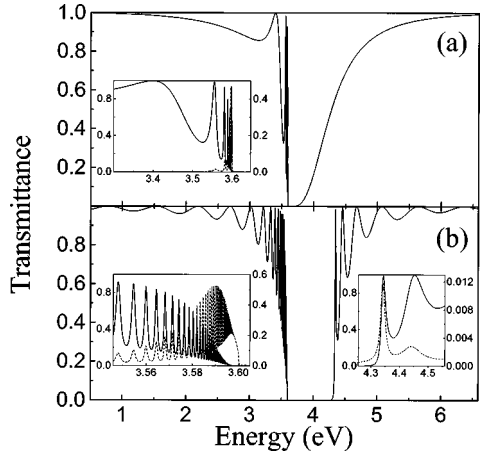

FIG. 6. Transmittance of light incident normally on a slab of 4 (a) and 32 (b) lattice planes parallel to the (001) surface of a fcc crystal consisting of plasma spheres ($S=50$ Å, $\hbar\omega_p=9.2$ eV, $\hbar\tau^{-1}=10^{-4}$ eV, $f=0.1$) in gelatine ($\epsilon=2.37$). In the insets we show the transmittance (solid line, read left axis) and absorbance (broken line, read right axis) in the immediate vicinity of the band gap edges. The results shown are obtained in the dipole approximation ($\ell_{\max}=1$).

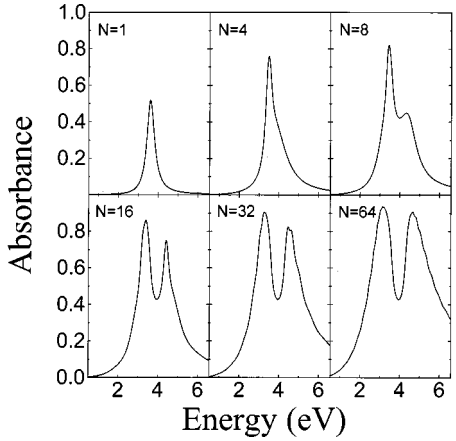

FIG. 7. Absorbance of light incident normally on a slab of N lattice planes parallel to the (001) surface of a fcc crystal consisting of plasma spheres ($S=50$ Å, $\hbar\omega_p=9.2$ eV, $\hbar\tau^{-1}=0.2$ eV, $f=0.1$) in gelatine ($\epsilon=2.37$).

In Fig. 6 we have deliberately used a rather small value of $\hbar\tau^{-1}=10^{-4}$ eV, in order to demonstrate the close relation between absorption and transmission. Let us next see what happens for a more realistic value of τ; we put $\hbar\tau^{-1}=0.2$ eV. When $\hbar\tau^{-1}$ becomes comparable with the energy interval between the peaks shown in Fig. 6, the peaks lose their discreteness, merging into broader peaks, with tails extending into what was (in the absence of absorption) a frequency gap. This is quite clearly seen by comparing the absorbance of the 4-layers and 32-layers slabs in Fig. 7 ($\hbar\tau^{-1}=0.2$ eV), with the absorbance of the same slabs in Fig. 6 ($\hbar\tau^{-1}=10^{-4}$ eV). The asymmetry between the high and low frequency peaks of the absorbance curves of Fig. 7 follows immediately from our analysis of the corresponding curves of Fig. 6. According to that analysis we expect this asymmetry to be less pronounced as the thickness of the slab increases, and this is what one sees in Fig. 7. At this stage we should emphasize that for the slabs considered (the values of the various parameters are summarized in the figure captions), there is no noticeable difference in the absorbance curves between the exact treatment and the effective-medium approximation. Absorption occurs over a range of frequencies about ω_1 [the dipole resonance of the sphere defined by Eqs. (7)], as shown in Fig. 7, but there is no significant absorption due to other bands (corresponding to ℓ-pole resonances, with $\ell>1$, of the sphere) as suggested in Ref. 3.

We have assumed so far that light is incident normally on the slab. A similar analysis can be carried through for any angle of incidence, or equivalently for any value of $\mathbf{k}_\parallel$ provided $|\mathbf{k}_\parallel|<\omega\sqrt{\epsilon}/c_0$ (see, e.g., Ref. 15). When $\mathbf{k}_\parallel\neq 0$ the nondegenerate bands, not shown in Fig. 1(a), which are in-

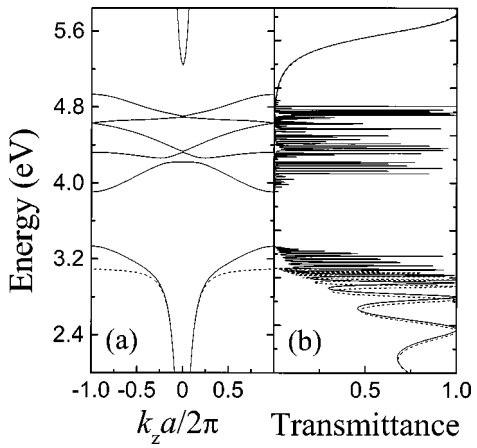

FIG. 8. (a) The photonic band structure associated with the (001) surface of a fcc crystal of nonabsorbing plasma spheres ($S=50$ Å, $\hbar\omega_p=9.2$ eV, $\tau=\infty$) in gelatine ($\epsilon=2.37$) with $f=0.3$, for $\mathbf{k}_\parallel=0$. (b) The corresponding transmittance curve for light incident normally on a slab of the above crystal, 16-layers thick. The solid (broken) lines in both figures refer to the exact (effective-medium) treatment.

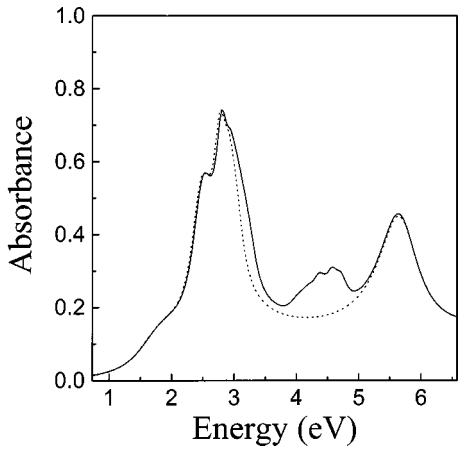

FIG. 9. Absorbance of light incident normally on a slab of 16 lattice planes parallel to the (001) surface of a fcc crystal consisting of plasma spheres ($S=50$ Å, $\hbar\omega_p=9.2$ eV, $\hbar\tau^{-1}=0.2$ eV, $f=0.3$) in gelatine ($\epsilon=2.37$). The solid (broken) line corresponds to the exact (effective-medium) treatment.

active for $\mathbf{k}_\parallel=0$, develop into bands which become *gradually* more active (couple with the externally incident light) as $|\mathbf{k}_\parallel|$ increases. However, their effect is marginal and the effective-medium treatment remains valid for practical purposes for the system considered in this section.

IV. FURTHER LIMITATIONS OF THE EFFECTIVE-MEDIUM APPROXIMATION

The effective-medium treatment, which effectively replaces the metallic spheres by interacting dipoles, breaks down when higher ($\ell>1$) than the dipolar ($\ell=1$) terms need to be taken into account for the description of the EM field about a sphere. This happens when the size of the spheres is large enough to activate absorption by ℓ-pole ($\ell>1$) resonances of the individual sphere, or when the fractional volume of the spheres increases. We note that similar deviations from the effective-medium treatment have been established for two-dimensional arrays of metallic spheres.[20]

In Fig. 8(a) we show the frequency band structure of a fcc crystal of nonabsorbing metal spheres ($S=50$ Å, $\hbar\omega_p=9.2$ eV, $\tau=\infty$) in gelatine ($\epsilon=2.37$) with a fractional volume occupied by the spheres $f=0.3$ (corresponding to a lattice constant $a=191.12$ Å), for $\mathbf{k}_\parallel=0$. Since the spheres are closer to each other as compared with the case examined in Sec. II ($f=0.1$), the band which arises from the interaction between dipole resonances of neighboring spheres is broader and hybridizes more strongly with the continuum states of the homogeneous effective background [Eq. (9)]. As a result of the stronger hybridization, a larger gap opens up and the higher-multipole ($\ell>1$) flat bands now fall into the gap region. Moreover, due to the larger overlap between resonant states of adjacent spheres, these flat bands are broader than in the case of $f=0.1$. We note that only doubly degenerate bands and up to $\ell_{\max}=4$ are shown in the figure. Figure 8(b) shows the corresponding transmittance curve, for light incident normally on a slab of the material 16-layers thick. One, now, can see the transmission resonances associated with the higher-multipole bands extending over a broad frequency region within the dipole gap. When absorption is switched on ($\hbar\tau^{-1}=0.2$ eV) these higher-multipole resonances are manifested as additional absorption peaks, as shown in Fig. 9.

We must also remember that we have assumed throughout the paper that the spheres are arranged periodically in space, and in particular we have assumed that the spheres are centered on the sites of a fcc lattice. Similar results are expected for any other cubic lattice. But for lattices of lower symmetry the effective-medium treatment we have presented will not be valid. A single dielectric function can not describe the optical properties of crystals of lower symmetry as is well known.[21] While it may be possible to develop an effective-medium treatment to calculate the principal values of the dielectric tensor (two for uniaxial crystals: rhombohedral, te-

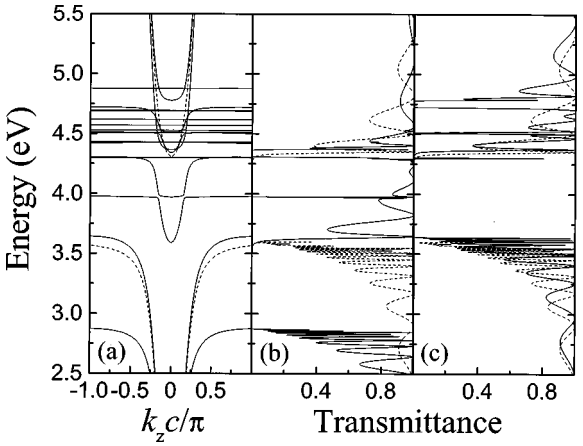

FIG. 10. (a) The photonic band structure associated with the (001) surface of an orthorhombic ($a:b:c=1:1.5:2$) crystal of nonabsorbing plasma spheres ($S=50$ Å, $\hbar\omega_p=9.2$ eV, $\tau=\infty$) in gelatine ($\epsilon=2.37$) with $f=0.1$, for $\mathbf{k}_\parallel=0$. (b) and (c) show the transmittance of light polarized in the x and y direction, respectively, incident normally on a 16-layers thick slab of the above crystal. The solid lines in the figures are exact results. The broken lines are obtained using the effective-medium formulas (3) and (5).

tragonal, and hexagonal systems, and three for biaxial systems: triclinic, monoclinic, and orthorhombic systems), we do not know that such a method exists at the present time and we cannot therefore say anything on this matter here. We simply mention that an effective-medium treatment for a general two-dimensional periodic system has recently been proposed by Halevi *et al.*[22] Our exact method works, of course, for any periodic arrangement of spheres and in order to demonstrate this we show in Fig. 10, the frequency band structure and the corresponding transmittance curves (for x and y polarized incident light) for an orthorhombic crystal. It is evident from this figure that x and y polarized incident light is coupled to different bands (nondegenerate in this case). One can easily recognize the nondegenerate bands, two below and two above the hybridization gap which correspond roughly to the doubly degenerate bands (one above and one below the gap) obtained in an effective-medium treatment based on Eqs. (3) and (5). These equations are obviously inappropriate in the present case and the corresponding bands are shown here only for comparison purposes. Of course, in the long wavelength limit (energy going to zero) the exact bands (solid lines) converge towards each other and to the effective-medium band (broken line).

Finally, we should mention that in practical applications the metallic particles (spheres) are rarely identical, and their arrangement in space is not always periodic. Although the main effect of disorder (at least of a mild one) is likely to be a broadening of the absorption peaks, a systematic treatment of disorder is a difficult mathematical problem and we shall deal with it in a subsequent publication.

ACKNOWLEDGMENT

V. Yannopapas was supported by the State Foundation (I.K.Y.) Greece.

*Electronic address: vyannop@atlas.uoa.gr

[1] S. Norrman, T. Andersson, and C. G. Granqvist, Phys. Rev. B **18**, 674 (1978).
[2] F Abelès, Y. Borensztein, and T. López-Rios, *Festkörperprobleme*, Advances in Solid State Physics Vol. 24 (Vieweg, Braunschweig, 1984), p. 93.
[3] J. B. Pendry, J. Mod. Opt. **41**, 209 (1993).
[4] A. R. McGurn and A. A. Maradudin, Phys. Rev. B **48**, 17 576 (1993).
[5] A. J. Sievers, in *Solar Energy Conversion*, edited by B. O. Seraphin (Springer, Berlin, 1979), p. 57.
[6] G. Mie, Ann. Phys. (Leipzig) **25**, 377 (1908).
[7] P. Debye, Ann. Phys. (Leipzig) **30**, 57 (1909).
[8] J. D. Jackson, *Classical Electrodynamics* (Wiley, New York, 1975).
[9] J. C. Maxwell Garnett, Philos. Trans. R. Soc. London, Ser. A **203**, 385 (1904); **205**, 237 (1906).
[10] A. Liebsch and B. N. J. Persson, J. Phys. C **16**, 5375 (1983).
[11] J. D. Joannopoulos, R. D. Meade, and J. N. Winn, *Photonic Crystals* (Princeton University Press, New York, 1995).
[12] *Photonic Band Gap Materials*, edited by C. M. Soukoulis (Kluwer Academic, Dordrecht, 1996).
[13] E. Yablonovitch, J. Phys.: Condens. Matter **5**, 2443 (1993).
[14] M. C. Wanke, O. Lehmann, K. Müller, Q. Wen, and M. Stuke, Science **275**, 1284 (1997).
[15] N. Stefanou, V. Karathanos, and A. Modinos, J. Phys.: Condens. Matter **4**, 7389 (1992).
[16] K. Ohtaka and Y. Tanabe, J. Phys. Soc. Jpn. **65**, 2276 (1996).
[17] N. Stefanou, V. Yannopapas, and A. Modinos, Comput. Phys. Commun. **113**, 49 (1998).
[18] W. M. Robertson, G. Arjavalingam, R. D. Meade, K. D. Brommer, A. M. Rappe, and J. D. Joannopoulos, Phys. Rev. Lett. **68**, 2023 (1992).
[19] V. Karathanos, J. Mod. Opt. **45**, 1751 (1998).
[20] N. Stefanou and A. Modinos, J. Phys.: Condens. Matter **3**, 8149 (1991); A. Modinos and N. Stefanou, Acta Phys. Pol. A **81**, 91 (1992).
[21] L. D. Landau, E. M. Lifshitz, and L. P. Pitaevskiĭ, *Electrodynamics of Continuous Media*, 2nd ed. (Butterworth-Heinemann Ltd., Oxford, 1984).
[22] P. Halevi, A. A. Krokhin, and Phys. Rev. Lett. **82**, 719 (1999).